FISCHER-TROPSCH SYNTHESIS IN SLURRY REACTOR SYSTEMS. QUARTERLY REPORT, MAY 1, 1984-JULY 31, 1984

MASSACHUSETTS INST. OF TECH., CAMBRIDGE

1984

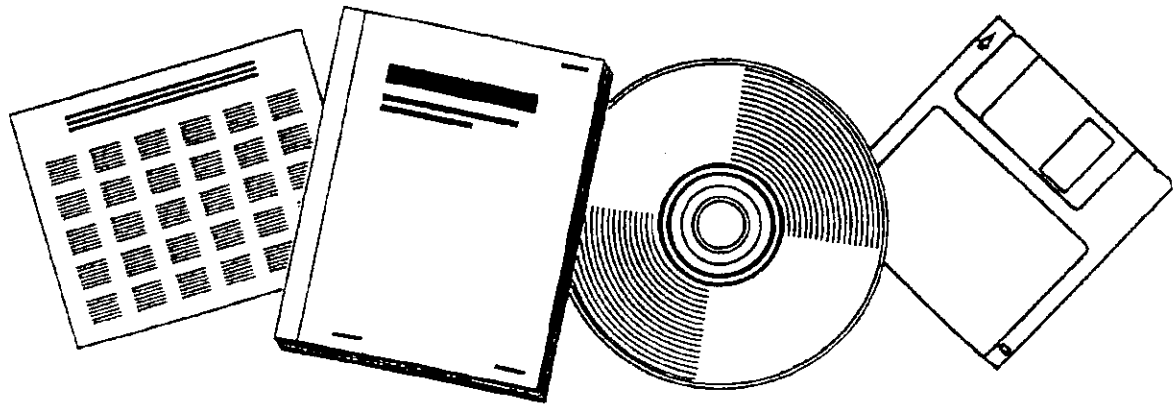

U.S. DEPARTMENT OF COMMERCE
National Technical Information Service

DOE/PC/40771-13
(DE84015438)
Distribution Category UC-90d

Fischer-Tropsch Synthesis in Slurry Reactor Systems

Quarterly Report for Period

May 1, 1984 to July 31, 1984

Department of Chemical Engineering

and

Energy Laboratory

Massachusetts Institute of Technology

Cambridge, Massachusetts

Report No.: DOE/PC40771-13

Grant No.: DE-FG22-81PC40771

Submitted by:

C.N. Satterfield

T. Bartos

R. Hanlon

G.A. Huff, Jr.

D. Matsumoto

I. SUMMARY

A. We suspect that a number of reports in the published literature of catalyst preparations that supposedly minimize wax formation are erroneous in that wax may actually have accumulated in catalyst pores and that insufficient time may have been allowed for the effluent to represent true intrinsic kinetics. We have now made a number of mathematical simulations to evaluate this effect and have prepared a paper for publication summarizing these studies. A copy is attached. An abstract is as follows:

Mathematical simulations show the effect of pressure, temperature, rate constant, feed composition, space velocity and Flory parameter α, on time required for pores to fill, upon liquid product distribution and vapor composition leaving the reactor. The pore filling rate and condensed product composition vary with position through the reactor but not with time. The maximum filling rate does not occur at the same position in the bed as the maximum synthesis rate. For reaction conditions of industrial interest, the greatest effect is caused by the assumed carbon number distribution of the products. A rigorous parameter to generalize the results is not immediately evident.

B. In the last quarterly we reported studies of the effect of the nature of the liquid on the activity and selectivity of a reduced fused magnetite catalyst. For interpretation of such studies it is necessary to have data on solubilities of hydrogen and carbon monoxide in the liquids of interest. We have made such measurements and have prepared a "communication" for publication summarizing the results. A copy is attached and an abstract is as follows:

New data at elevated temperatures and pressure are reported for octacosane, phenanthrene and Fomblin, a perfluorinated polyether, and compared to previous literature on a variety of liquids. When hydrogen solubilities are reported on a volumetric basis, substances of a similar chemical nature have very similar solubilities.

LIQUID ACCUMULATION IN CATALYST PORES IN A FISCHER-TROPSCH FIXED-BED REACTOR

George A. Huff, Jr., and Charles N. Satterfield
Department of Chemical Engineering
Massachusetts Institute of Technology
Cambridge, MA

ABSTRACT

Mathematical simulations show the effect of pressure, temperature, rate constant, feed composition, space velocity and Flory parameter α, on time required for pores to fill, upon liquid product distribution and vapor composition leaving the reactor. The pore filling rate and condensed product composition vary with position through the reactor but not with time. The maximum filling rate does not occur at the same position in the bed as the maximum synthesis rate. For reaction conditions of industrial interest, the greatest effect is caused by the assumed carbon number distribution of the products. A rigorous parameter to generalize the results is not immediately evident.

INTRODUCTION

Products ranging from methane to high molecular-weight hydrocarbons are synthesized from carbon monoxide and hydrogen during the Fischer-Tropsch reaction over a variety of catalysts. In a fixed bed reactor at representative process conditions, higher molecular weight products will condense in the reactor and fill the pores of the catalyst.

The accumulation of non-volatile liquid, essentially a paraffin wax, within the catalyst bed presents two problems. First, the effluent product distribution upon bringing a fresh catalyst on stream will be biased initially

towards the lighter, more volatile products until steady state is attained when catalyst pores in the reactor become filled with liquid product and external liquid holdup likewise reaches steady state. Some claims in the literature of Fischer-Tropsch products deviating from the Flory carbon number distribution may result from insufficient time having been allowed for steady-state to be reached. Second, the liquid wax may inhibit the rate of reaction by slowing reactant mass transfer within the catalyst pores (Anderson, et al., 1964). Reportedly, the removal of this liquid product by periodic in-situ extraction with a lighter solvent made possible increased activity of German fixed-bed reactors packed with either iron or cobalt catalysts (Anderson, 1956). Even though this same phenomenon is observed for SASOL fixed-bed reactors, they are not washed with solvent because the pores refill with wax quickly after such treatment and the period of high activity is thus short lived (Dry, 1981).

In this paper, we present mathematical analyses to predict pore filling effects in a fixed-bed Fischer-Tropsch reactor utilizing a porous catalyst. The results of the simulation are presented which show how the distribution of products in the reactor effluent is predicted to vary with time and process variables such as catalyst activity and selectivity, temperature, and pressure. A similar analysis for a slurry reactor system has recently been reported by Huff (1982) and Dictor and Bell (1983), but the behaviour of the two kinds of systems differs because they accumulate product in different ways.

MODEL DEVELOPMENT

Consider a fixed-bed reactor operating in plug flow and containing catalyst particles with initially empty pores. Synthesis gas is fed continuously to the reactor while volatile products and unconsumed reactants leave in the effluent vapor and heavier products condense as liquid in the catalyst pores.

Intrinsic Product Distribution. Before an expression can be derived to relate the distribution of product between vapor and liquid phases, the composition of products actually being formed on the catalyst across the bed length must be determined. The analysis uses reaction kinetics and product carbon number distributions typical of iron catalysts but the results provide guidance as to the general behaviour that may occur with catalysts that behave differently.

In general, the stoichiometry of the Fischer-Tropsch synthesis on iron may be expressed as:

$$j\ CO + 2J\ H_2 \rightarrow C_jH_{2j} + j\ H_2O \qquad (1)$$

where the average organic product is assumed to be a hydrocarbon designated "C_jH_{2j}." The water-gas-shift reaction, which is very fast over iron, is assumed to equilibrate under synthesis conditions (Huff and Satterfield, 1984a:)

$$H_2O + CO = CO_2 + H_2 \qquad (2)$$

With the stoichiometry of Eq. 1 and 2, the conversion of reactants and formation of products can be estimated throughout a fixed-bed reactor upon assuming that the rate of synthesis gas consumption is dependent only on the hydrogen concentration to the first order (Huff and Satterfield, 1984a:)

$$-R_{H_2+CO} = kP_{H_2} \qquad (3)$$

The actual rate of product synthesis of carbon number n is determined in the following manner. First, the stoichiometric coefficient j is predicted by the Flory expression for the average molecular weight, MW, of product "C_jH_{2j}." On several iron catalysts the molecular weight distribution corresponds to the sum of two chain-growth probabilities, α_1 and α_2, where $\alpha_1 < \alpha_2$. The α_1 distribution dominates up to about C_{10} and the α_2 at higher C numbers (Huff and Satterfield, 1984b).

In that event,

$$MW = 14j = 14Z/(1-\alpha_1) + 14(1-Z)/(1-\alpha_2) \quad (4)$$

where Z is the mole fraction of product produced by the α_1 distribution. The overall rate of formation of total organic "C_jH_{2j}" is estimated from eq. 3. This value is multiplied by the mole fraction m_n of the total organic that corresponds to carbon number n, to give the rate of formation of product of carbon number n, m_n, as:

$$m_n = Z(1-\alpha_1)\alpha_1^{n-1} + (1-Z)(1-\alpha_2)\alpha_2^{n-1} \quad (5)$$

If the catalyst should exhibit only a single value of α, then Eq. 4 and 5 are modified by substituting $\alpha_1 = \alpha$ and $Z = 1$, so the second term in both equations disappears.

Assumptions. The following simplifying assumptions are made: (i) Diffusion of reactants into and product out of catalyst pores occurs fast enough to neglect mass transfer resistances. (ii) The liquid phase is considered to be ideal. The vapor-liquid equilibrium distribution for each carbon number product is represented by Raoult's law. (iii) The reactor bed is isothermal and isbaric. (Most of the heat generated in the reactor comes from the highly exothermic synthesis step; the heat of total product condensation is more than 50-fold smaller.) (iv) The variation of vapor pressure with surface curvature because of capillary pore size is neglected, as suggested by the following example. If the pores of a fused-iron catalyst are taken to be cylindrical with a diameter of 40 nm (Anderson, 1956) and the liquid completely wets the surface, then we estimate from the Kelvin equation that the vapor pressure for a C_{30} hydrocarbon would be reduced by less than 20% at 225°C because of capillary curvature. (v) The catalyst instantaneously attains constant activity and selectivity upon start-up and maintains this same level of performance over the course of the reaction. (iv) Only

products from C_1 through C_{100} are considered. (We found no significant change in the predicted results when products beyond C_{75} are neglected for distributions that follow the Flory equation.) Products are assumed to be linear paraffins. (vii) The catalyst particles are assumed to have the same pore volume throughout the bed.

Note that our analysis is valid only up to the time that the first catalyst pore fills completely with liquid anywhere in the reactor. We do not consider vapor-liquid exchange or other effects once liquid begins trickling down the reactor. This time thus represents the minimum time for the products leaving the reactor to exhibit their intrinsic distribution.

Material Balance Equations. For calculational purposes, a finite-element method is applied to simulate the fixed-bed reactor in which the condensation of products is a function of both axial position and time. The reactor is approximated as a finite number of continuous stirred-tank reactors (termed elements) that are operating in an unsteady-state condition. The total number of elements is chosen such that convergence and stability of the finite-element approximation is attained. For our analysis, the catalyst bed was subdivided axially into 50 elements, which gave essentially the same results as several cases in which far fewer elements were used.

A material balance written for product of carbon number n around the catalyst particles contained in element m gives:

$$\underset{\text{synthesized}}{r_{n,m}} = \underset{\substack{\text{Liquid Accumulation}\\ \text{in Pore}}}{d(x_{n,m})/dt} + \underset{\substack{\text{Vapor Flow}\\ \text{Output}}}{y_{n,m}} - \underset{\substack{\text{Vapor Flow}\\ \text{Input}}}{y_{n,m-1}} \qquad (6)$$

where product accumulation in the vapor phase of the reactor is neglected. Vapor-liquid equilibrium is attained within each pore of catalyst contained in element m so that Raoult's law can be expressed as:

$$(y_{n,m})P_t/G_m = (x_{n,m})P_n^{VP}/X_m \tag{7}$$

where $x_m = \sum_{n=1}^{100} x_{n,m}$ and $G_m = [(\sum_{r=1}^{100} y_{n,m}) +$ total molar flow rate of unconsumed reactants, carbon dioxide, and water]. Combining eq. 6 and 7 yields:

$$d(x_{n,m})/dt = r_{n,m} + \frac{x_{n,m-1}P_n^{VP}G_{m-1}}{X_{m-1}P_t} - \frac{x_{n,m}P_n^{VP}G_m}{X_m P_t} \tag{8}$$

Initially, the pores are completely empty so that the boundary condition is $x_{n,m} = 0$ and $t = 0$, and the feed is pure synthesis gas so that $y_{n,0} = 0$.

G_0 = molar flow rate of hydrogen and carbon monoxide fed to the reactor. Since the contribution of hydrocarbon product to the total molar flow is small (see eq. 1 and 2), the total molar flow (G_m for element m) used is that for the intrinsic distribution of products and reactants in which condensation is neglected.

Considering the wide range of carbon numbers synthesized, eq. 8 represents a series of first-order equations that must be solved simultaneously for each element because of their interdependence on X_m. However, if the rate of total liquid accumulation dX_m/dt is taken to be independent of time, then:

$$X_m = A_m t \tag{9}$$

where A_m is a constant representing the total rate of liquid accumulation within element m. The consequences of this assumption are discussed in Appendix A. Substitution of eq. 9 into eq. 8 and integration gives:

$$x_{n,1} = \frac{r_{n,1}A_1 t}{(P_n^{VP}G_1/P_t + A_1)} \quad \text{for } m = \tag{10}$$

Combination of eq. 8 through 10 upon integration yields:

$$x_{n,2} = \frac{A_2\left\{r_{n,2} + \dfrac{P_n^{VP}G_1 r_{n,1}/P_t}{(P_n^{VP}G_1/P_t + A_1)}\right\} t}{(P_n^{VP}G_2/P_t + A_2)} \quad \text{for } m = 2 \tag{11}$$

The procedure is successively repeated along the bed length for the remaining elements.

Given the input variables (such as G_0, k, etc.), the dependence of pore filling on time and axial position in the reactor bed is simulated as follows: Proceeding from the first element, the constant A_m for each element m is obtained by applying the expression for $x_{n,m}$ (eq. 10 or 11) for n = 1 to 100 and solving it iteratively with the definition for X_m that:

$$X_m = \sum_{n=1}^{100} x_{n,m} = A_m t \qquad (12)$$

The value of A_m is adjusted until satisfactory convergence is obtained. Values of P_n^{vp} are estimated by the Antoine equation from coefficients given by Zwolinski and Wilhoit (1971). The volume of liquid in the pores of element m is estimated by correcting the molar amounts $x_{n,m}$ with density, based on data from API Research Project 44. The calculational strategy involves starting with the pores initially empty and incrementing time until any one of the elements in the bed is predicted to be completely filled with liquid, at which time the computation is stopped. This final time is called the pore-filling time.

RESULTS AND DISCUSSION

In order to understand the physical significance of some of the results predicted by the mathematical analysis, we consider first a set of base conditions, summarized in Table I, and then examine the singular effect of varying pressure, temperature, rate constant, space velocity, feed ratio (H_2/CO), and α value. The range of reaction variables used for illustration are typical of those for a fixed-bed reactor containing an iron catalyst promoted with potassium. A shift in the dominating distribution at a carbon number of about 10 corresponds to Z = 0.95 (Huff and Satterfield, 1984b).

General Form of Results. Consider first the base conditions given in Table I. For the temperature, pressure and space velocity specified, conversions of H_2 and CO are 23% and 35%, respectively. For this case, the synthesis rate (eq. 3) is relatively constant through the bed. The first pores to completely fill anywhere in the catalyst bed do so at a predicted time of 311 min. Figure 1 presents a plot of both the volume percent of pores occupied by liquid product and the average molecular weight of condensed liquid versus axial position in the reactor at this time. The fractional volume of liquid contained in the first element (which represents 2% of the catalyst bed for 50 total elements) at the inlet is extrapolated to zero for a bed length of zero (represented by a dashec line in Figure 1) because the feed contains only pure reactant gases. The increase in degree of pore filling progressively along the catalyst bed is caused by a greater fraction of lighter products condensing, as evidenced by the decrease in average molecular weight with length, shown in Figure 1. This effect is further illustrated by Figure 2 which shows how the product distribution in the liquid varies with axial position at the moment of first pore filling.

Figure 3 depicts the ratio of product of carbon number n in the vapor to total product of carbon number n versus n at the moment of first pore filling, for three different positions in the catalyst bed. At 263°C and 790 kPa products with a carbon number below about 30 are too volatile ever substantially to condense whereas those above about 70 remain mostly as liquid. For product of a given carbon number in the range of about C_{35} to C_{60}, the degree of condensation increases with axial distance, which accounts for the porefilling profiles observed in Figures 1 and 2. These intermediate-range products remain mostly as vapor in catalyst pores located near the reactor inlet where the incoming vapor-phase concentration of these

products is still small. However, with increased distance through the bed a greater fraction condense because their amount is larger from intrinsic catalytic production and the total moles of gas present is smaller from consumption of reactants (eq. 1 and 2). Simply put, as the term $y_{n,m}/G_m$ grows through the bed, Raoult's law (eq. 7) dictates that the value of $x_{n,m}$ increases, which corresponds to more of these intermediate-range products condensing as liquid.

Figure 4 is a plot of the logarithm of fraction of total organic product of carbon number n in the vapor versus n for different positions across the catalyst bed. An increasingly larger fraction of the products fall below the Flory line further away from the inlet. This is a result of the increased condensation of products through the bed, as explained above.

The carbon number distributions in Figures 2 through 4 correspond to that determined from the time reaction is started with empty pores to the moment that the first pore is completely filled with liquid. The distributions change with position through the bed but not with time, as shown in the Appendix. Figure 4 shows that the steady-state distribution of products in the effluent vapor (fractional distance of 1.0) while the pores are filling, is markedly different from that actually synthesized by the catalyst per the Flory equation (eq. 5). To properly characterize the intrinsic performance of the catalyst, it is critical then that either experiments be conducted at times long enough to obtain the intrinsic product distribution in the reactor effluent or condensed liquids must be properly accounted for by recovery and analysis.

Effect of Total Pressure. The conversion of carbon monoxide and distribution of liquid in the pores at the time of filling are plotted versus bed length at pressures of 445, 790, and 1480 kPa in Figure 5. It is not surprising that the porefilling profiles are essentially the same because the intrinsic carbon number distribution of products per the Flory equation is the same for all three pressures. In accordance with Raoult's law (eq. 7), more

light products are condensed at higher pressures as evidenced by the curves of average molecular weight of condensed liquid presented in Figure 6.

The predicted times for filling the first pores as pressure is changed are summarized in the first section of Table II. The time is shortest at the highest pressure of 1480 kPa for two reasons: products are formed more rapidly (eq. 3); and they are less volatile (eq. 7). Both factors are important. If the increased rate of hydrocarbon synthesis were the sole determining factor, then the filling time would be inversely proportional to inlet hydrogen partial pressure, P_{H_2} (eq. 3) since the rate is relatively constant over the bed. This latter observation is manifested by a constant slope for curves of percent CO conversion versus bed length in Fig. 5. On this basis the time to fill the pores at 1480 kPa would be approximately $[(P_{H_2})_{445\ kPa}/(P_{H_2})_{1480\ kPa}] \times (time)_{445\ kPa} =$ $[(211)/(701)]709 = 213$ min. When compared to the results at 445 kPa, the time actually predicted is much lower, 129 min., indicating that increased condensation of lighter products at the higher pressure is quite important. Hence, the effects of both the intrinsic reaction rate and relative volatility must be taken into account when interpreting pore-filling results upon changing the total pressure.

Effect of Temperature. Profiles of carbon monoxide conversion and liquid filling at temperatures of 232, 248, and 263°C are illustrated in Figure 7. The degree of condensation of liquid in pores along the bed is relatively unaffected by temperature because the distribution of products per the Flory equation is unaltered. This is analogous to the constant behaviour observed upon changing total pressure. The vapor pressure of the hydrocarbon product increases slightly with temperature so fewer light products are condensed. Thus the average molecular weight of liquid in the pores increases slightly with temperature (Figure 8).

The predicted times for filling the first pores as temperature are changed are summarized in the second section of Table II. The time is shortest at the highest temperature of 263°C, at which the intrinsic rate of product synthesis is fastest. This factor outweighs the fact that products are more volatile. If the increased intrinsic rate were the overwhelming factor, then the filling time would be inversely proportional to the intrinsic rate constant k. The time for pore filling at 263°C would then be approximately $(k_{232°C}/k_{263°C}) \times (\text{time})_{232°C} = (0.71/2.2)922 = 298$ min., compared to the results at 232°C. This rough estimate is surprisingly close to the predicted filling time of 311 min., which indicates that increase in volatility at higher temperatures is a minor effect compared with the increase in intrinsic reaction rate. Figure 8 confirms this conclusion because the average molecular weight of condensed liquid, an indicator of volatility, is observed to be nearly independent of temperature.

Effect of Rate Constant

The less active the catalyst, the longer the time required for the first pores to fill completely but this time is not inversely proportional to k. This is shown in Table 2 for the base case.

Effect of H_2/CO Feed Ratio

The time for first pore filling will decrease with increased (H_2/CO) feed ratio since the rate is proportional to hydrogen partial pressure and is relatively constant over the bed. However, again the relationship is not linear, in part because of variations in the average molecular weight of condensed product with bed length. Some representative results are shown in Table II for the base case.

Effect of Space Velocity: Up to this point, the results are for a constant space velocity. At the highest pressure and temperature considered, the CO

conversion was only 64%. We now consider a wide range of degree of conversion.

The predicted variations of pore filling and carbon monoxide conversion with space velocity are shown in Figures 9 and 10, respectively. The curves in Figure 9 are fairly similar for space velocities of 1500 cm^3 gas (S.T.P.)/ h-g cat. and greater, in which carbon monoxide conversion is incomplete. For lower space velocities, carbon monoxide conversion is complete and the maximum rate of pore filling occurs at an intermediate position along the bed and not at or near reactor outlet, as it does for lower CO conversions. As suggested by Eq. 8, the effect from the change in rate of product formation with length opposes that for the process by which more material is condensed. As a result, even though the maximum rate of reaction occurs at the reactor inlet where the hydrogen partial pressure is highest (Eq. 3), the rate of pore filling continues to increase through the bed until most of the carbon monoxide is consumed (the maximum rate occurs at about 80% CO consumption for the cases considered in Figure 9).

The times required to fill the first pores as space velocity is changed are given in Table II. For space velocities below about 2000 cm^3 gas (S.T.P.)/ h-g cat., the times are about the same at 275 min., which is explained as follows. First, the average molecular weights of the condensed product at the point of maximum pore filling are about the same at 540 g/mol for these cases (see Figure 11). Second, the amount of product intrinsically synthesized is the same because rate of reaction is unchanged with both constant values of k and hydrogen partial pressure. However, since the average molecular weight of condensed product is considerably higher at higher space velocities, the times for first pore filling are longer (Table II) even though the intrinsic rate of reaction is constant.

Effect of carbon number distribution. This is discussed in terms of the Flory parameter α. The effect of α on pore filling is shown in Figures 12-15, assuming

that the intrinsic carbon number distribution is represented by a single value of α. Figure 12 shows that the α value significantly changes the rate of pore filling at each element and that the profile flattens as the value of α increases. At larger values of α, the product is heavier and mostly remains as condensed liquid in the pore in which it is formed, so that the effect of saturation/condensation through the bed is less pronounced. Similarly, the average molecular weight of liquid product becomes more uniform through the reactor bed (Figure 13). As the value of α increases, the time to fill the first set of pores decreases since the product is less volatile (Figure 14). However, the time markedly increases at α greater than about 0.97. While the product is still becoming heavier, the average molecular weight is now quickly approaching infinity such that much fewer moles of products are synthesized. Whether this is realistic physically is problematical.

Figure 14 explains the observation by Dry (1981) that in the SASOL fixed bed reactors the pores of the iron catalyst become filled within "minutes" of startup. The product from these reactors corresponds to $\alpha = 0.87$ to 0.90, and they operate at about 220 to 240°C and 2.6 MPa pressure.

Figure 15 shows the time required to fill the first pore as a function of α for various combinations of temperature and pressure of interest. The reaction conditions are for the base case of Table 1, except that various values of a single α are considered. In general, when α is less than about 0.80 to 0.85, the time required to fill the first pore is longer than that typical of most laboratory experiments and it becomes exceedingly sensitive to α.

Carbon Number Distribution in Vapor

It becomes evident that the products can be divided into three groups: (1) those that are found essentially in the vapor after a short period; (2) those that distribute between vapor and liquid in pores; and (3) those that exist

essentially as liquid. The boundaries between these groups obviously depend on many variables but in general for the reaction conditions of interest (200-300°C and 500-2000 kPa), products below about C_{25} to C_{30} will be adequately represented by a vapor-phase analysis after a short unsteady state period, those above about C_{60} will never be found significantly in the vapor.

The intermediate region, about C_{30} to C_{60}, is the most sensitive to reaction conditions. Figure 16 gives some additional guidance. It presents the molecular weight distribution of the vapor at the moment of first pore filling for several combinations of pressure and temperature. The base case of Table 1 is again taken, with a single α value of 0.85.

Falsification of α_2. Figure 4 shows that while liquid is accumulating in the pores of the catalyst, the vapor phase product for higher carbon number material corresponds to a straight line on a Flory plot, from which a value of α_2 considerably less than the true value would be calculated. The reason for this behaviour lies in the happenstance that the logarithm of the vapor pressure of linear paraffins at constant temperature varies inversely with carbon number n, i.e.,

$$p_n^{vp} = C_1 \beta^n \tag{13}$$

where C_1 is a constant and β is the slope of the curve. As shown in Appendix B for higher carbon number product, the mole fraction of C_n in the organic product vapor, $Y_{n,m}$ is:

$$Y_{n,m} \propto (\beta \cdot \alpha_2)^n \tag{14}$$

where α_2 is the true value of α_2 and the product $\beta \cdot \alpha$ is that observed. Values of β are relatively insensitive to temperature, varying from 0.69 at 232°C to 0.74 at 263°C. (See Figure 17.) For ~ ideal solution behaviour, β is independent of pressure. In Figure 4, the apparent α based on the vapor at the bed exit

(1.0 fractional distance) and n greater than about 40 is 0.70, whereas the true α is 0.93. This is consistent with Eq. 14 where the expected value is $\beta\alpha_2$ = (0.93)(0.74) = 0.69.

CONCLUSIONS

As a consequence of accumulating liquid products in the catalyst pores, the product distribution in the vapor phase after starting a fixed-bed Fischer-Tropsch reactor will exhibit an absence of heavy products. As time progresses, the vapor phase composition is predicted to be unchanged until the first pore completely fills. Beyond this point, the observed distribution will become progressively more characteristic of the intrinsic catalyst behaviour as liquid oozes out of the pores and begins to trickle down to the reactor exit.

The filling of catalyst pores with liquid is complex. Several principal conclusions about this phenomenon are reached based on the simplified mathematical analyses presented in this paper: (1) The rate of filling of catalyst pores varies with position through the reactor but not with time, up to the time the first pore is completely filled. (2) The maximum rate of filling of pores does not occur at the same position in the bed as the maximum rate of synthesis. (3) The product composition in the catalyst pores varies with position in the bed but not with time, until the first pore is completely filled. (4) While all the pores fill with liquid, the intrinsic product distribution may be such that the time required may be on the order of minutes or so long as to approach infinity.

Several simulations of the effect of reaction variables such as pressure, temperature, etc., on pore filling provide guidance in design and interpretation of data: (1) A change in pressure affects volatility and intrinsic rate. Both factors significantly affect pore-filling behaviour. (2) The major effect of changing temperature is that it changes the synthesis rate; volatility is of